

Electronic Supporting Information for:

Synthesis and Self-Assembly of a Mikto-Arm Star Dual Drug Amphiphile Containing both Paclitaxel and Camptothecin

Andrew G. Cheetham^{†,‡}, Pengcheng Zhang[†], Yi-an Lin^{†,‡}, Ran Lin[†], and Honggang Cui^{*,†,‡}

[†]Department of Chemical and Biomolecular Engineering, and [‡]Institute for NanoBioTechnology (INBT), Johns Hopkins University, Baltimore, Maryland 21218, USA

Email: hcui6@jhu.edu

Table of Contents

S1. Synthesis of the Dual Drug Amphiphiles	S3
S1.1 Chemical & technical abbreviations	S3
S1.2 Materials and methods	S3
S1.3 Characterization of the dual drug amphiphiles	S4
S1.4 Drug loading calculations	S6
S1.5 Drug amphiphile concentration assay	S6
S1.6 Reactivity of CPT-Cys-Sup35 and PTX-Cys-Sup35	S7
S2. Self-Assembly Characterization	S9
S2.1 Effect of dilution into PBS on CPT-PTX-Sup35 assembly.....	S9
S2.2 Cryo-TEM images of dCPT-Sup35	S9
S2.3 Nanostructure Stability	S10
S2.3.1 CD study on the effect of dilution on nanostructure stability	S10
S2.3.2 Critical aggregation concentration (CAC) determination of CPT-PTX-Sup35	S10
S2.3.3 Hydrolytic stability of the assembled structures.....	S11
S3. Drug Release HPLC Protocol.....	S12
S4 Cytotoxicity	S13
S4.1 Full cytotoxicity protocol.....	S13
S4.2 Cytotoxicity results	S13
S4.3 dCys-Sup35 cytotoxicity	S14

S1. Synthesis of the Dual Drug Amphiphiles

S1.1 Chemical & technical abbreviations

CPT - camptothecin

DA – drug amphiphile

DMSO – dimethylsulfoxide

Fmoc - fluorenylmethyloxycarbonyl

HATU – *O*-(7-azabenzotriazol-1-yl)-*N,N,N',N'*-tetramethyluronium hexafluorophosphate

HBTU – *O*-(benzotriazol-1-yl)-*N,N,N',N'*-tetramethyluronium hexafluorophosphate

MALDI-ToF – matrix-assisted laser desorption/ionization time-of-flight

MeCN – acetonitrile

MS – mass spectrometry

PBS – phosphate-buffered saline

PTX – paclitaxel

RP-HPLC – reverse-phase high performance liquid chromatography

TCEP – tris(carboxyethyl)phosphine

TFA – trifluoroacetic acid

S1.2 Materials and methods

Fmoc amino acids and coupling reagents (HBTU or HATU) were purchased from Advanced Automated Peptide Protein Technologies (AAPPTEC, Louisville, KY, USA), with the exception of Fmoc-Lys(Fmoc)-OH which was obtained from Novabiochem (San Diego, CA, USA). Rink Amide MBHA resin was purchased from Novabiochem (San Diego, CA, USA). Camptothecin and paclitaxel were purchased from AvaChem Scientific (San Antonio, TX, USA) and all other reagents were sourced from Sigma-Aldrich (St. Louis, MO) or VWR (Radnor, PA, USA), unless otherwise stated.

RP-HPLC was performed on a Varian ProStar Model 325 HPLC (Agilent Technologies, Santa Clara, CA, USA) equipped with a fraction collector. Preparative separations utilized a Varian PLRP-S column (100 Å, 10 µm, 150 × 25 mm), whilst analytical HPLC used a Varian Pursuit XRs C18 column (5 µm, 150 × 4.6 mm). Water and acetonitrile containing 0.1% v/v TFA were used as the mobile phase. Purified molecules were lyophilized on a FreeZone –105°C 4.5 L freeze dryer (Labconco, Kansas City, MO, USA). MALDI-ToF mass spectrometric data was acquired on an Autoflex III Smartbeam (Bruker, Billerica, MA, USA) using α -cyano-4-hydroxycinnamic acid as the matrix.

S1.3 Characterization of the dual drug amphiphiles

dCPT-Sup35: the lyophilized powder was dissolved in 3 mL H₂O. Calibration based on the CPT absorbance gave a conjugate concentration of 448 μ M. Yield = 3.2 mg, 10%. MS (MALDI-ToF): 2407.293 [M+H]⁺; MS (ESI): 1204.2 [M+2H]²⁺, 1215.3 [M+H+Na]²⁺, 1226.3 [M+2Na]²⁺;

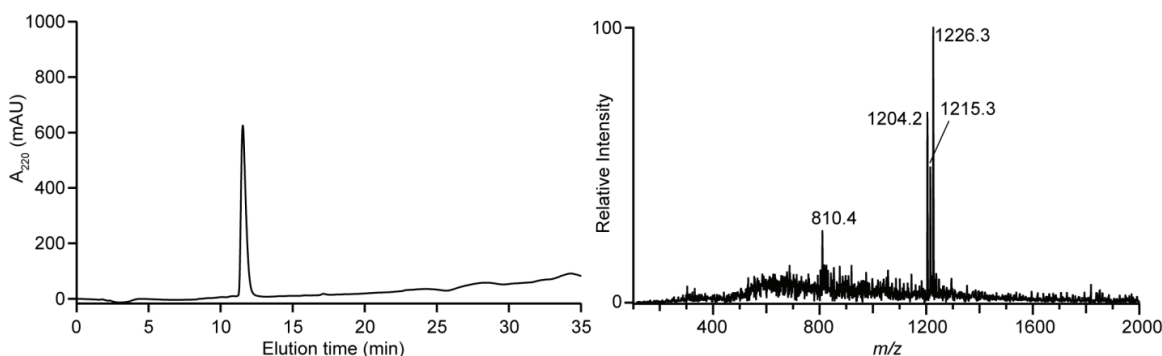


Fig. S1 HPLC chromatogram (left) and ESI-MS spectrum (right) of purified **dCPT-Sup35**.

CPT-PTX-Sup35: the lyophilized powder was dissolved in 6 mL of 1:1 MeCN/H₂O. Calibration based on the CPT absorbance gave a conjugate concentration of 400 μ M. Yield = 7.0 mg, 17%. MS (MALDI-ToF): 2912.822 [M+H]⁺; MS (ESI): 1457.0 [M+2H]²⁺, 1468.4 [M+H+Na]²⁺, 1478.9 [M+2Na]²⁺.

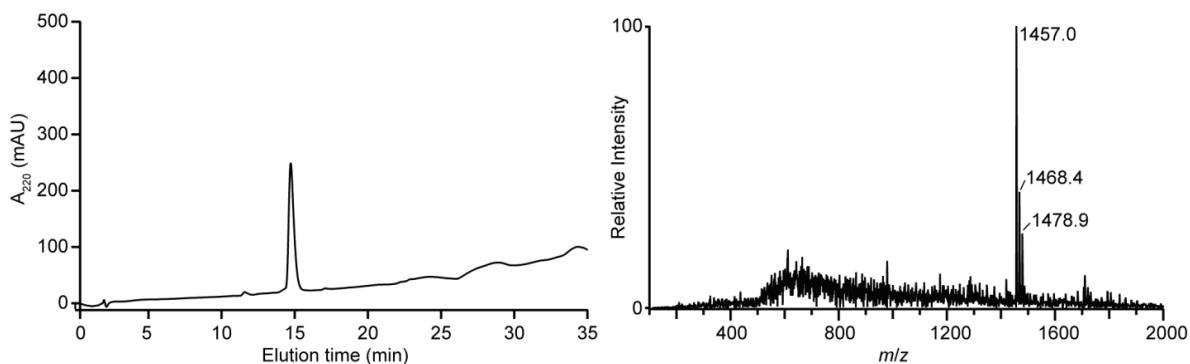


Fig. S2 HPLC chromatogram (left) and ESI-MS spectrum (right) of purified **CPT-PTX-Sup35**.

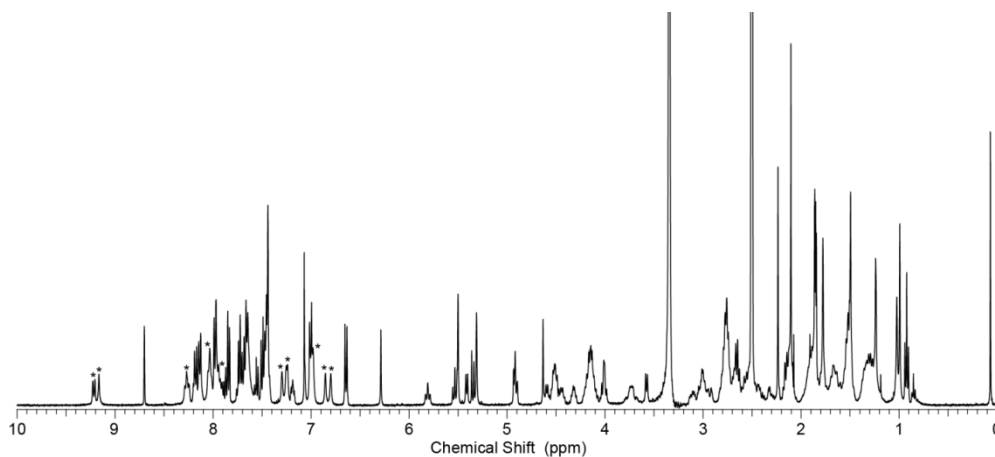


Fig. S3 ^1H NMR ($\text{D}_6\text{-DMSO}$, 400 MHz) of **CPT-PTX-Sup35** (exchangeable amide protons as determined by the addition of a small amount of D_2O are indicated by *).

dPTX-Sup35: the lyophilized powder was dissolved in 3 mL of 1:2 MeCN/ H_2O . Calibration based on the PTX absorbance gave a conjugate concentration of 204 μM . Yield = 2.1 mg, 4%. MS (MALDI-Tof): 3418.988 $[\text{M}+\text{H}]^+$.

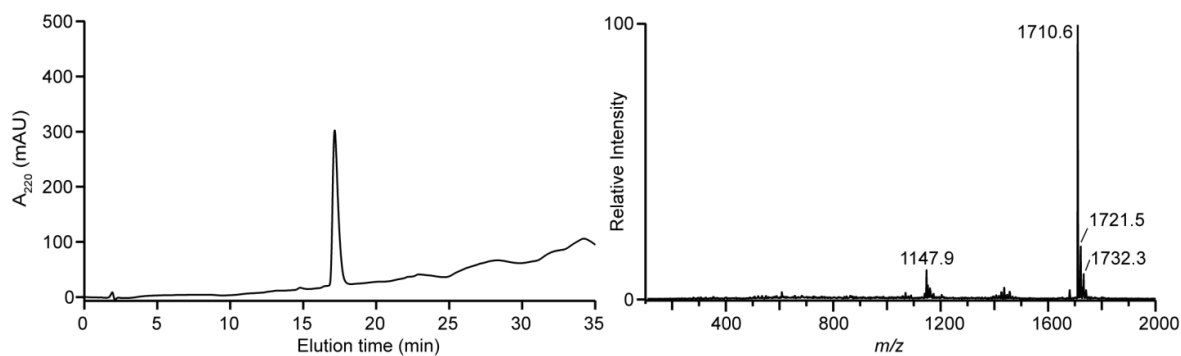


Fig. S4 HPLC chromatogram (left) and ESI-MS spectrum (right) of purified **dPTX-Sup35**.

S1.4 Drug loading calculations

The drug loading of the drug amphiphiles is given as the drug weight as a percentage of the total molecular weight:

$$\text{Drug loading (\%)} = \frac{M_{\text{Drug}}}{M_{\text{DA}}} \times 100$$

where M_{Drug} is the exact mass of the drug (CPT or PTX) and M_{DA} is the exact mass of the drug amphiphile

$$\text{CPT-PTX-Sup35 CPT drug loading (\%)} = \frac{1 \times 347.1}{2911.1} \times 100 = 12\%$$

$$\text{CPT-PTX-Sup35 PTX drug loading (\%)} = \frac{852.3}{2911.1} \times 100 = 29\%$$

$$\text{Total drug loading (\%)} = 12 + 29 = 41\%$$

S1.5 Drug amphiphile concentration assay

To determine the CPT concentration of the purified drug amphiphiles, a TCEP reduction assay was developed. Briefly, 25 ml of an aqueous acetonitrile solution (1:1 H₂O/MeCN) of the conjugate with an approximate concentration in the range 5 to 500 μM was treated with 25 ml of a freshly prepared 1 M aqueous TCEP solution and allowed to stand at least 1 h with periodic vortexing. 30 μL of this sample were then mixed with 20 μL of DMSO and analyzed by RP-HPLC, measuring the area of the peak due to **CPT-buSH**. The CPT concentration of the analyzed solution in μM was determined using a calibration curve of TCEP-reduced **CPT-buSS-Pyr**). The conjugate concentration of the original solution was calculated based on the applied dilutions and number of CPT molecules the conjugate possesses.

S1.6 Reactivity of CPT-Cys-Sup35 and PTX-Cys-Sup35

To demonstrate that the conjugates were isolated as free and reactive thiols, they were tested for their ability to undergo disulfide exchange, both with themselves (Fig. S5) and with other reactive species (Fig. S5). **CPT-Cys-Sup35** was initially dissolved in water and immediately analyzed by HPLC, showing that the dominant species was still the isolated product (black trace in Fig. S5). After 1 h, the formation of **dCPT-Sup35** and **CPT-buSH** could be seen (blue trace in Fig. S5), indicating that the conjugate's free thiol was acting as a nucleophile toward **CPT-Cys-Sup35**. Diluting a portion of the solution into PBS, it was clear that the higher pH enabled the thiol to become more active as the extent of reaction was more pronounced (red trace in Fig. S5), giving the disulfide, **(CPT-buS)₂** as the dominant species. These observations are as expected given thiols become more reactive at higher pH, with the aqueous and PBS solutions having pH values of ~5 and 7.4, respectively.

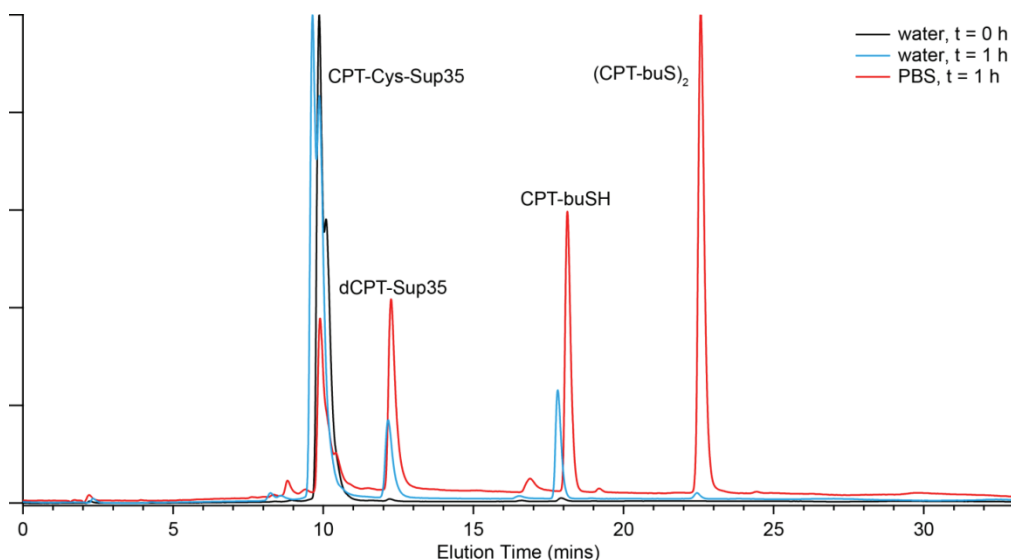


Fig. S5 HPLC analysis of an aqueous solution of **CPT-Cys-Sup35** upon initial dissolution (black) and after 1 h (blue). The aqueous solution was also diluted two times into PBS and monitored after 1 h. Both solutions shows that the **CPT-Cys-Sup35** will scramble to give **dCPT-Sup35**, **CPT-buSH** and **(CPT-buS)₂**, with the speed of reaction determined by the solution pH (~5 for water and 7.4 for PBS). Chromatograms are normalized with respect to the most intense signal.

A DMSO solution of **PTX-Cys-Sup35** was allowed to react with the activated disulfide, **CPT-buSS-Pyr**, giving the hetero-DDA, **CPT-PTX-Sup35**, as the major product (Fig. S6). This and the previous

experiment both illustrate the potential usefulness of a singly reacted di-thiol containing species, as it can be isolated and then used as a reagent to form other dual drug amphiphiles as desired.

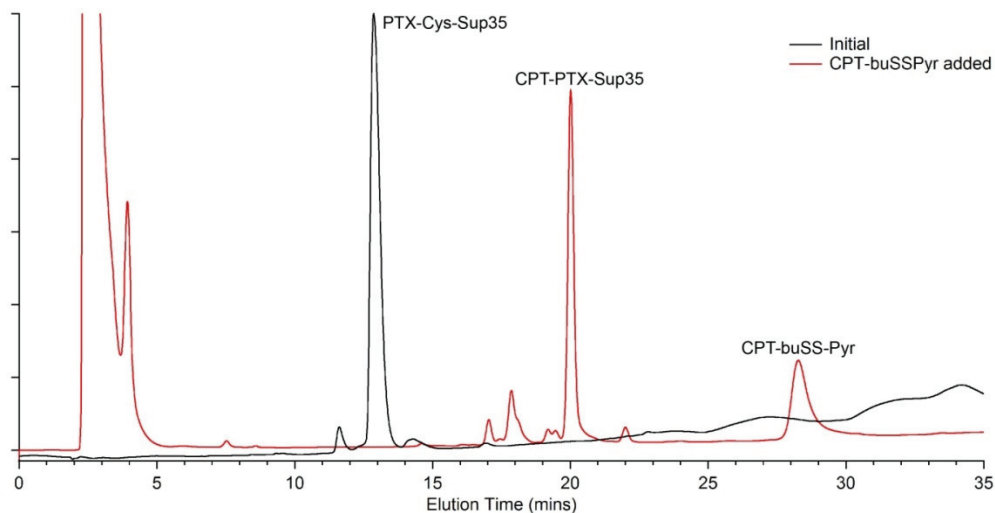


Fig. S6 HPLC analysis of a DMSO solution of **PTX-Cys-Sup35** to which was added **CPT-buSS-Pyr**, indicating that the conjugate remains active towards directed disulfide exchange and allows formation of the **CPT-PTX-Sup35** dual drug amphiphile. This suggests that the singly reacted species can be isolated and used as a reagent in its own right for the reaction with other activated drug molecules.

S2. Self-Assembly Characterization

S2.1 Effect of dilution into PBS on CPT-PTX-Sup35 assembly

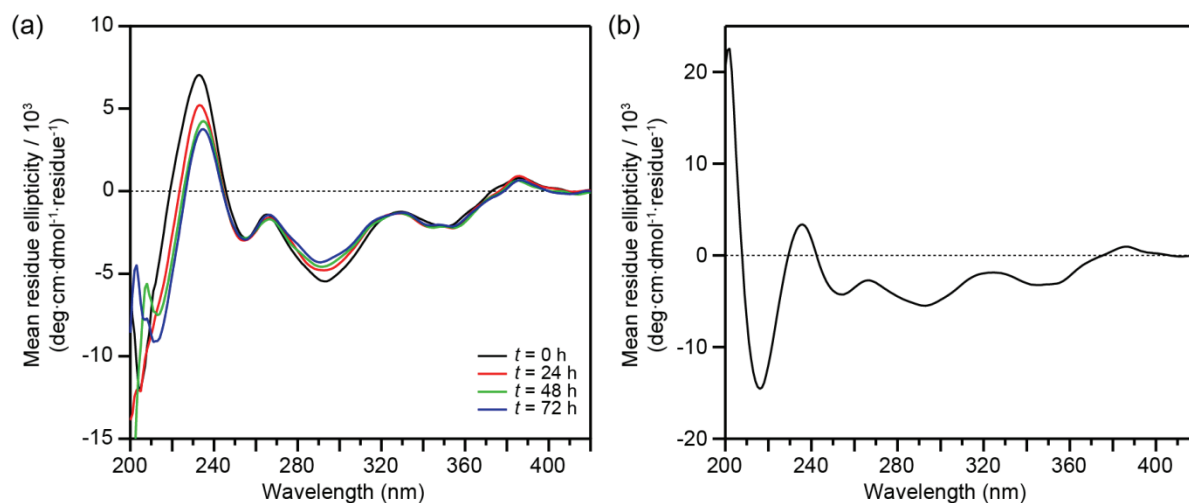


Fig. S7 Effect of dilution into PBS on the self-assembly of **CPT-PTX-Sup35**. (a) Time course study of a $100 \mu\text{M}$ sample in PBS prepared from a 1 mM solution in water that had been aged for 2 h, showing the slow evolution of the β -sheet signal. (b) The CD spectra of a $100 \mu\text{M}$ sample in PBS prepared from a 1 mM solution in water that had been aged for 8 d, indicating that dilution into PBS does not disrupt the matured nanostructure.

S2.2 Cryo-TEM images of dCPT-Sup35

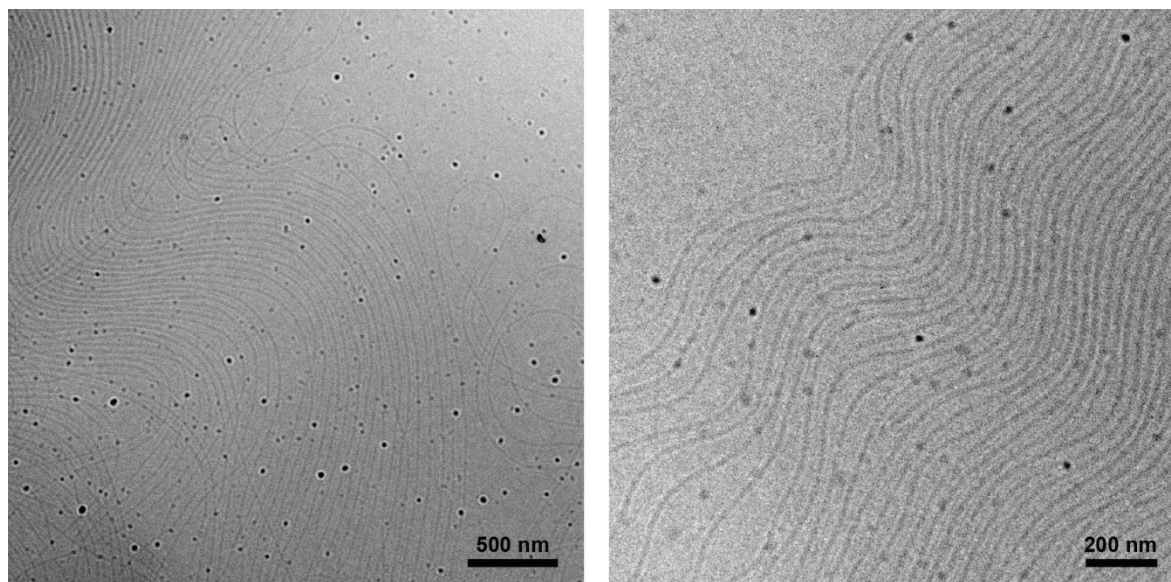


Fig. S8 Representative cryo-TEM images of a $500 \mu\text{M}$ aqueous solution of **dCPT-Sup35**. The dark spheres are caused by ice crystals in the vitreous ice film and were formed during sample preparation.

S2.3 Nanostructure Stability

S2.3.1 CD study on the effect of dilution on nanostructure stability

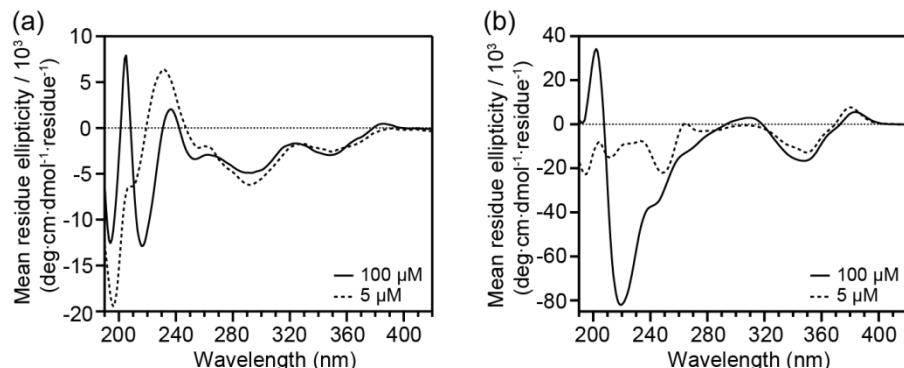


Fig. S9 Circular dichroism spectra of 100 μM (aged overnight, filled line) and 5 μM (recorded after dilution of the 100 μM sample, dotted line) solutions of **CPT-PTX-Sup35** (a) and **dCPT-Sup35** (b)..

S2.3.2 Critical aggregation concentration (CAC) determination of CPT-PTX-Sup35

The CAC values for **CPT-PTX-Sup35** and **dCPT-Sup35** were determined using a Nile Red encapsulation method. Briefly, from a 1 mM stock of **CPT-PTX-Sup35** or **dCPT-Sup35** in water that had been aged for at least 2 days, a series of dilutions in pure water were prepared, ranging from 0.5 nM to 200 μM . To 250 μL of each solution, was added 2.5 mL of a 1 mM solution of Nile Red in acetone. The acetone was then allowed to evaporate and the solution was equilibrated overnight. The fluorescence spectrum of each solution was recorded using a Fluorolog spectrofluorometer (Horiba Jobin Yvon Inc., Edison, NJ), exciting at 550 nm and collecting the emission intensity between 580 and 720 nm. To obtain the CAC value, the data from the 640 emission was plotted against the concentration on a log scale, with the value given by the intersection of the two linear segments (Fig. S10). The experiment was repeated to verify the trend.

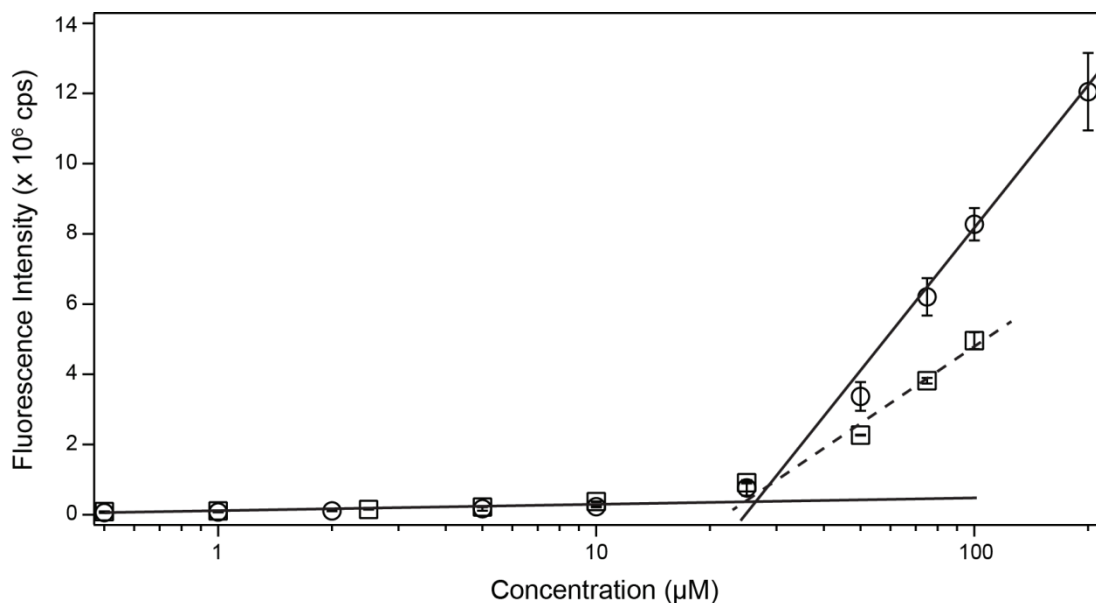


Fig. S10 Critical aggregation concentration (CAC) determination of CPT-PTX-Sup35 (○) and dCPT-Sup35 (□) using a Nile red fluorescence method. Data are given as mean \pm s.d. ($n = 2$).

S2.3.3 Hydrolytic stability of the assembled structures

The hydrolytic stability of the assembled DAs was determined by analysis of 100 μ M and 1 mM solutions after 2 weeks of aging at room temperature.

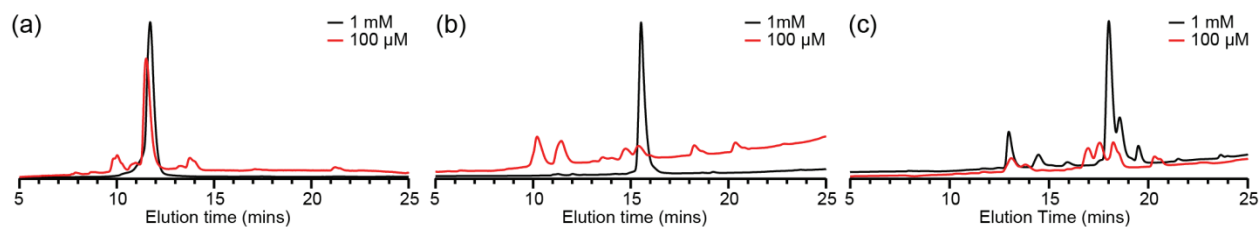


Fig. S11 Hydrolytic stability of dCPT-Sup35 (a), CPT-PTX-Sup35 (b), and dPTX-Sup35 (c) at 100 μ M (red trace) and 1 mM (black trace) in pure water after 2 weeks aging at room temperature. All solutions were monitored using a wavelength of 220 nm.

S3. Drug Release HPLC Protocol

The degradation of CPT-PTX-Sup35 was monitored by RP-HPLC using the following conditions: 237 nm detection wavelength; 1 ml/min flow rate; mobile phase was 0.1% aqueous TFA (A) and acetonitrile containing 0.1% TFA; gradient is given in Table S1. The concentrations of **CPT-PTX-Sup35**, CPT and PTX were determined by measuring the area of the respective peaks and comparing against a calibration curve for each species.

Table S1 HPLC gradient used for drug release study.

Time (min)	Mobile Phase A (%)	Mobile Phase B (%)
0	65	35
5	65	35
18	13	87
21	13	87
22	65	35
25	65	35

S4 Cytotoxicity

S4.1 Full cytotoxicity protocol

KB-3-1 or KB-V1 were seeded onto 96-well plate (5×10^3 cells/well) and allowed to attach overnight. **PTX-CPT-Sup35** was diluted with fresh medium and incubated with cells immediately to achieve final conjugate concentrations. Medium containing the same concentration of PTX, CPT or **dPTX-Sup35** were also used to incubate the cells, with non-treated cells (solvent only) as the control group. After 48 h incubation, the cell viability was determined using the SRB method according to the manufacturer's protocol (TOX-6, Sigma, St. Louis, MO).

S4.2 Cytotoxicity results

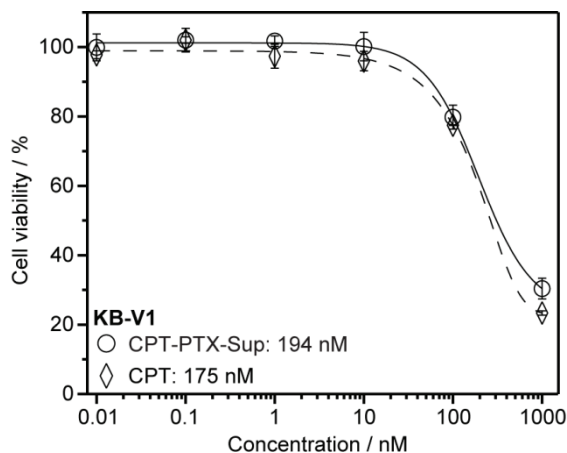


Fig. S12 Comparison of the cytotoxicity of **CPT-PTX-Sup35** and CPT against PTX-resistant KB-V1 cervical cancer cells. Cell viability was determined by SRB assay after 48 h incubation with the appropriate drug-containing media. Calculated IC_{50} values are given in the figure legends, data are given as mean \pm s.d. ($n = 3$).

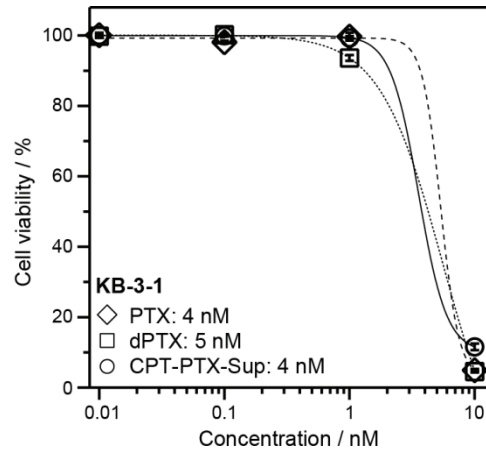


Fig. S13 Cytotoxicity study of PTX, CPT-PTX-Sup35 and dPTX-Sup35 against PTX-sensitive KB-3-1 cervical cancer cells. Cell viability was determined by SRB assay after 48 h incubation with the appropriate drug-containing media. Calculated IC₅₀ values are given in the figure legends, data are given as mean ± s.d. (*n* = 3).

S4.3 dCys-Sup35 cytotoxicity

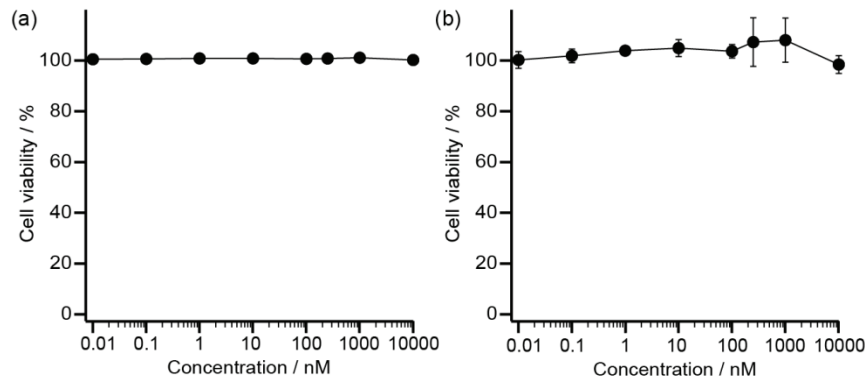


Fig. S14 Cytotoxicity of dCys-Sup35 against KB-3-1 (a) and KB-V1 (b) cervical cancer cells. Cell viability was determined by SRB assay after 48 h incubation with the appropriate drug-containing media. Data are given as mean ± s.d. (*n* = 3).